# Voltage distribution in a two-component random system

Andrzej Kolek
*Department of Electrical Engineering, Rzeszów University of Technology, Wincentego Pola 2, 35-959 Rzeszów, Poland*
(Received 4 May 1995; revised manuscript received 18 December 1995)

A disordered medium composed of randomly arranged metal and insulator, both with finite conductance, is considered. The distribution of voltage drops $v$ in such two-component random system has been calculated both analytically and numerically. It is shown that the distribution $N(y)$ of the logarithm of voltage drops, $y=-\ln(v^2)$, is the sum of several members, $N_{ck}(y)$ and $N_{ik}(y)$, $k=0,1,2,\ldots$. Members $N_{ck}(y)$ describe the voltage distribution in the metallic phase. Members $N_{ik}(y)$ describe the voltage distribution in the insulating component. The subsequent members are shifted subsequently on the $y$ axis by an amount of $2k\ \ln(hL^{1/(\nu\varphi)})$, where $\varphi$ is the crossover exponent and $\nu$ is the percolation correlation length exponent. The zero-order member of the $N_{ck}$ family is governed by the multifractal spectrum $f(\alpha)$, where $\alpha=y/\ln L$, found originally for the random resistor network. The zero-order member of the $N_{ik}$ family is governed by the multifractal spectrum $\phi(\alpha)$ found originally for the random resistor superconductor network. The next members are built from two components. The first one is the scaled repetition of $N_{c0}$ for the $N_{ck}$ family or $N_{i0}$ for the $N_{ik}$ family. The other one is the distribution of voltage drops in such percolation objects like dangling ends, isolated clusters for the $N_{ck}$ family or clusters perimeter for the $N_{ik}$ family.

## I. INTRODUCTION

Transport properties of heterogeneous media have recently attracted much interest because of their relevance to many industrial applications. When the disorder of the medium is extremely large, percolation theory[1] is a very efficient tool of investigation. The properties of electrical transport can be then described by the distribution of voltage drops in the so-called random resistor network (RRN). It turns out that various moments of this distribution have physical interpretations.[2–4] For example, the zero moment describes the mass of the percolating backbone, the second one is the network conductance, the fourth is related to resistance $1/f$ noise whereas the infinite moment is governed by the so-called singly connected bonds,[1–5] i.e., those carrying the largest current in the percolating cluster. It was shown that at the percolation threshold all positive moments of voltage distribution scale as power laws of system size $L$ but with different exponents.[2–4,6] This leads to the conclusion that the voltage distribution in RRN has a multifractal structure.[2,3,7–9] The term ''multifractal'' means that there is an infinite (continuous) set of irrelevant exponents $f(\alpha)$ which describe the power-law scaling, as a function of system size, of different regions $\alpha$ of the distribution. The multifractal spectra were found for the two ideal random resistor networks. For RRN, i.e., for the network in which ideal insulator $g_i=0$ and normal conductor (metal) are mixed, the spectrum $f(\alpha)$ which describes scaling of voltage distribution within the metal was found.[3,7–14] For random resistor superconductor network (RRSN), i.e., the network in which the ideal conductor $g_c=\infty$ is diluted in the host of the normal metal, the spectrum $\phi(\alpha)$ which describes scaling of the voltage distribution again in metal was also found.[3] Although in both cases the spectra describe scaling of the voltage distribution in the metallic phase, they are related to different geometrical objects. In the case of RRN the spectrum refers to percolating cluster whereas for RRSN it refers to the ''rest'' of the lattice. For dimensions $d>2$ those two are different geometrical objects and thus the spectra have different shapes for RRN and RRSN, i.e., $f\neq\phi$ for dimensions $d>2$.

RRN and RRSN may be considered as the limiting cases of the more general two-component random resistor network (TCRRN) in which both components of the mixture take finite values of the conductance.[15] This is also a more realistic model of the metal-insulator composite in which nonzero conductivity of an insulator is taken into account. Alternatively, it is also a more realistic model of the mixture of metal and real superconductor with small but nonzero resistivity. After some controversy[16] it was argued that moments of voltage distribution in the two-component RRN crossover from fractal to homogeneous region with the *single crossover exponent* associated with the ratio $h$ of the conductance of the components, $h=g_i/g_c$, irrespective of the moment's order.[17–23] This conclusion leads to important and nontrivial results concerning the behavior of various physical quantities in inhomogeneous systems. For example, it was shown that new critical exponents control the dependence of $1/f$ noise intensity on mixture composition in the vicinity of the percolation threshold.[17–23] Thus the investigations of voltage distribution in the two-component RRN are very important. While the first attempt suggests the distribution to be approximately Gaussian[24] our present results do not confirm this conclusion. We have found that the distribution of the logarithm of voltage drops $v$ is composed of several peaks shifted subsequently on the $y=-\ln(v^2)$ axis by an amount of $2\ \ln(hL^{1/(\nu\varphi)})$, where $\varphi$ and $\nu$ are the crossover exponent and the percolation correlation length exponent, respectively.

The rest of the paper is organized as follows: In Sec. II we shortly review the multifractal approach to voltage distribution in RRN and RRSN. In Sec. III the scaling functions for moments of current and voltage distributions are introduced and their new properties are established based on the usual scaling assumption. In Sec. IV the voltage distribution in the

 

two-component RRN is calculated via the inverse Laplace transform technique as proposed by Fourcade and Tremblay.[9] In Sec. V the alternative derivation of this distribution is given by the use of the hierarchical model of the two-component random system recently proposed by Morozovsky and Snarskii.[17,23] In Sec. VI a large number of computer simulations performed on a three-dimensional 3D simple cubic lattice is presented to show how the scaling theory predictions work in real TCRRN. Conclusions and remarks on topological interpretation of the obtained distribution are given in Sec. VII.

## II. MULTIFRACTAL APPROACH

Consider the RRN in which bonds are occupied with probability $p$ by unit conductance. With probability $1-p$ bonds are removed. For such a network moments of voltage distribution may be defined

$$W_q=\sum_b \left(\frac{V_b}{V}\right)^{2q}, \tag{1}$$

where $V_b$ denotes voltage drop on bond $b$ when external voltage $V$ is imposed to the network and summation is over all occupied bonds with nonzero voltages. Some of the above moments have physical interpretations. For example, the network conductance $G$ is just the first $(q=1)$ moment, $G=W_1$. Moments for $q=0$, $q=2$, and $q=\infty$ have also physical interpretations as was mentioned in the Introduction. Above the percolation threshold $p_c$ and for $L\to\infty$, $G$ reaches the thermodynamic limit and depends on $\varepsilon\equiv p-p_c$ and $L$ according to the well-known percolation power law[15]

$$G\sim\varepsilon^t L^{d-2}, \tag{2}$$

where $t$ is the conductivity exponent. At the percolation threshold, however, the percolation correlation length $\xi$ diverges and relation (2) is never approached, the system is always in the fractal (self-similar) region.[1] In this case the dependence of conductance $G$ on size $L$ can be obtained by putting $\varepsilon\sim\xi^{-1/\nu}=L^{-1/\nu}$ into Eq. (2), $\nu$ is the correlation length exponent.[1] Thus for $p=p_c$, $W_1\sim L^{-t/\nu+d-2}$. In general all positive moments defined in Eq. (1) scale with $L$ as power laws,[2,3,7]

$$W_q\sim L^{-p(2q)/\nu} \tag{3}$$

for $q\geqslant 0$. Above we use the notation of Refs. 2, 3, and 7. Note that it is completely equivalent to define the problem in terms of current distribution. Exponents $-x_q$ which describe the $L$ dependence of the moments of current distribution[4,6]

$$M_q=\sum_b \left(\frac{I_b}{I}\right)^{2q}\sim L^{-x_q},$$

where $I_b$ is the current in bond $b$ when external current $I$ biases the network, are then related to exponents $p(2q)/\nu$

$$x_q=\frac{p(2q)}{\nu}-2q\frac{p(2)}{\nu}.$$

It was shown that exponents $p(2q)/\nu$, or $x_q$, form an infinite set of independent exponents.[2–4,6–9] Some of them are well known. For example, $-p(0)/\nu=-x_0=D_B$ is the fractal dimension of the percolating backbone whereas $-p(2q)/\nu+2qp(2)/\nu=-x_\infty=1/\nu$ for $q\to\infty$. In the thermodynamic limit the $\varepsilon$ dependence of $W_q$ can be easily obtained if we note that for $L\gg\xi$ moments $W_q$ should scale as $(L/\xi)^{-2q}(L/\xi)^d\xi^{-p(2q)/\nu}$. Thus for $\xi\sim\varepsilon^{-\nu}$

$$W_q\sim L^{d-2q}\varepsilon^{t(2q)},$$

where exponents[3]

$$t(2q)=(d-2q)\nu+p(2q), \quad t(2)\equiv t. \tag{4}$$

Moments $W_q$ can be also expressed in terms of voltage distribution. Let $n(v^2)$ be the number of bonds with voltage drop $V_b=vV$. Then

$$W_q=\int_0^1 dv^2 n(v^2)v^{2q}. \tag{5}$$

The asymptotic form of $n(v^2)$ can be derived by the method proposed by Fourcade and Tremblay.[9] Namely Eq. (5) rewritten in terms of new variable $y=-\ln(v^2)$,

$$W_q=\int_0^\infty dy N_{\mathrm{RRN}}(y)\exp(-qy), \tag{6}$$

where $|N_{\mathrm{RRN}}(y)dy|=|n(v^2)dv^2|$, may be now considered as the Laplace transform of $N_{\mathrm{RRN}}(y)$, i.e., the distribution of the logarithm of voltage drops. Hence $N_{\mathrm{RRN}}(y)$ can be obtained by inverting Eq. (6). Using the saddle-point approximation they have shown that

$$N_{\mathrm{RRN}}(y)\sim L^{f(\alpha)}, \tag{7}$$

where $\alpha=y/\ln L=-\ln(v^2)/\ln L$ and $f(\alpha)$ is the Legendre transform of $p(2q)/\nu$, i.e., $(1/\nu)[\partial p(2q)/\partial q]=\alpha$, $f(\alpha)=q\alpha-p(2q)/\nu$. The above equation reads that for $\alpha$ fixed, $f(\alpha)$ may be interpreted[3,7] as a fractal dimension of a set of bonds characterized by a voltage drop that scales with size as $v^2\sim L^{-\alpha}$. $f(\alpha)$ is thus a continuous spectrum of fractal dimensions which characterize different parts $\alpha$ of the distribution of the logarithm of voltage drops in the network. Note that $f(\alpha)=D_B$ for $q=0$ and this is the maximum value of $f(\alpha)$ since any set of bonds characterized by a given voltage drop is always a subset of the percolating backbone.

Similarly we can describe multifractal properties of RRSN, i.e., the network in which bonds are occupied by superconductors (infinite conductance) with probability $p$. With probability $1-p$ bonds take unit conductance. Moments of voltage distribution are then defined by Eq. (1) but with summation extended over all (unoccupied) bonds with finite (unit) conductance over which nonzero voltages are observed. This change makes the critical exponents in RRSN different (for $d>2$) from that of RRN. At $p=p_c$ and for $q\geqslant 0$ moments $W_q$ scale as[3]

$$W_q\sim L^{\zeta(2q)}, \tag{8}$$

whereas for $p<p_c$ and $L\to\infty$ they crossover to

$$W_q\sim L^{d-2q}|\varepsilon|^{s(2q)-2qs}, \tag{9}$$

where

$$s(2q)-2qs=(d-2q)\nu-\zeta(2q)\nu,\ \ s(2)\equiv s. \quad (10)$$

Note that $s(2)=s$ is the conductivity critical exponent in RRSN, $\zeta(0)=d$, and $\zeta(\infty)=1/\nu$. The latter describes scaling of the number of singly disconnected bonds.[5,25] The distribution of the logarithm of voltage drops in RRSN is thus

$$N_{\mathrm{RRSN}}(y)\sim L^{\phi(\alpha)}, \quad (11)$$

where $\phi(\alpha)$ is the Legendre transform of $-\zeta(2q)$, i.e., $-\partial\zeta(2q)/\partial q=\alpha$, $\phi(\alpha)=q\alpha+\zeta(2q)$. As we have already pointed out the spectra $f$ and $\phi$ refer to different (for $d>2$) objects and in general they have different shapes.

## III. MULTIFRACTAL MOMENTS IN THE TWO-COMPONENT RRN

Let us consider the random resistor network in which the effect of nonzero conductance of the insulating phase is taken into account. In this network the ratio of ''poor'' $g_i$ and ''good'' $g_c$ conductance is given by a small-value parameter $h=g_i/g_c$. Conductance $g_c$ occupies bonds of $d$-dimensional lattice with probability $p$. Conductance $g_i$ occupies bonds with probability $1-p$. For such TCRRN moments of current and voltage distributions should be defined separately for the insulating ($i$) and conducting ($c$) bonds[17–21,23]

$$M_{iq}=\sum_b\left(\frac{I_b}{I}\right)^{2q},$$

$$W_{iq}=\sum_b\left(\frac{V_b}{V}\right)^{2q},$$

$$M_{cq}=\sum_b\left(\frac{I_b}{I}\right)^{2q},$$

$$W_{cq}=\sum_b\left(\frac{V_b}{V}\right)^{2q},$$

where $I_b(V_b)$ denotes current (voltage drop) in bond $b$, which belongs to either ($i$) or ($c$) phase, when external current $I$ (voltage $V$) is imposed on the network. All the next results are based on the natural assumption that in the thermodynamic limit each of the moments defined above is a *generalized homogeneous function* in the neighborhood of the point $h=0$, $\varepsilon=p-p_c=0$, i.e., near the percolation transition. Important are relations

$$W_{iq}=\left(\frac{G}{g_i}\right)^{2q}M_{iq},$$

$$W_{cq}=\left(\frac{G}{g_c}\right)^{2q}M_{cq}, \quad (12)$$

where $G$ is the conductance of the network. Some of the features of defined quantities can be easily established. For $h\to 0$ and $\varepsilon>0$ we get RRN and thus $W_{cq}\sim\varepsilon^{t(2q)}, M_{cq}\sim\varepsilon^{t(2q)-2qt}$. Similarly for $h\to 0$ and $\varepsilon<0$ we get RRSN and $M_{iq}\sim|\varepsilon|^{s(2q)}, W_{iq}\sim|\varepsilon|^{s(2q)-2qs}$. Let us now make the usual scaling hypothesis for each of the moments defined above. First let us draw our attention to the insulating phase:[21]

$$M_{iq}=M_{iq}(\varepsilon,h)=|\varepsilon|^{s(2q)}m_{iq}(h/|\varepsilon|^{1/\varphi}),$$

$$W_{iq}=W_{iq}(\varepsilon,h)=|\varepsilon|^{s(2q)-2qs}w_{iq}(h/|\varepsilon|^{1/\varphi}),$$

where $\varphi$ is the crossover exponent. It was proven that $\varphi$ takes unique value $\varphi=1/(t+s)$ for all multifractal moments independent of the moments order, i.e., for all $q\geqslant 0$.[17–21,23] Note that for $h=0$ moments $M_{iq}$ are defined both above and below $p_c$. $M_{iq}(\varepsilon,0)=0$ for $\varepsilon>0$ and $M_{iq}(\varepsilon,0)\sim|\varepsilon|^{s(2q)}$ for $\varepsilon<0$. If we further assume that $M_{iq}$ is singular only at $h=0,\varepsilon=0$, then for fixed finite $\varepsilon$, $M_{iq}$ is not singular and may be expanded about the point $h=0$,[26]

$$M_{iq}(\varepsilon,h)=M_{iq}(\varepsilon,0)+\sum_{k=1}^{\infty}\frac{1}{k!}\left.\frac{\partial^k M_{iq}}{\partial h^k}\right|_{h=0}h^k. \quad (13)$$

Now let us note that for $\varepsilon>0$ the conducting percolating cluster exists and all the currents in the insulating phase scale as $I_b=g_iV_b\sim g_iV\sim g_iI/G\sim g_iI/(g_c\varepsilon^t)\sim hI$. Consequently the leading term in $M_{iq}$ scales as $h^{2q}$, and this means that the first $2q-1$ derivatives in Eq. (13) vanish. Thus we get $M_{iq}$ expanded up to the first nonvanishing term

$$\begin{aligned}M_{iq}(\varepsilon,h)&=M_{iq}(\varepsilon,0)\\&\quad+h^{2q}|\varepsilon|^{s(2q)-2q/\varphi}\frac{1}{(2q)!}\left.\frac{\partial^{2q}m_{iq}(x)}{\partial x^{2q}}\right|_{x=0}\\&=M_{iq}(\varepsilon,0)+C'_{1q}h^{2q}|\varepsilon|^{s(2q)-2q/\varphi}.\end{aligned}$$

Moments $W_{iq}$ can now be calculated by the use of Eq. (12). For $\varepsilon<0$ we have $G\sim g_i|\varepsilon|^{-s}$ and

$$W_{iq}(\varepsilon,h)\sim|\varepsilon|^{s(2q)-2qs}+C_{1q}h^{2q}|\varepsilon|^{s(2q)-2q/\varphi-2qs}.$$

Note that for $\varepsilon<0$ we get $W_{iq}(\varepsilon,0)\sim\varepsilon^{s(2q)-2qs}$ as we expect, according to Eq. (9). The latter expression also reads that in the expansion of $W_{iq}(\varepsilon,h)$ about $h=0$ the first $2q-1$ derivatives, $\partial^k W_{iq}/\partial h^k$, vanish at $h=0$. Thus the above equation is valid also for $\varepsilon>0$. This leads us to the second nonvanishing term in Eq. (13). For $\varepsilon>0$ we get

$$\begin{aligned}M_{iq}(\varepsilon,h)&\sim h^{2q}|\varepsilon|^{s(2q)-2q/\varphi}+C'_{2q}h^{4q}|\varepsilon|^{s(2q)-4q/\varphi}=|\varepsilon|^{s(2q)}\\&\quad\times\{(h/|\varepsilon|^{1/\varphi})^{2q}+C'_{2q}(h/|\varepsilon|^{1/\varphi})^{4q}\}.\end{aligned}$$

If repeated this leads us to the conclusion that $m_{iq}$ and $w_{iq}$ are functions of $(h/|\varepsilon|^{1/\varphi})^{2q}$ rather than of $h/|\varepsilon|^{1/\varphi}$,

$$W_{iq}(\varepsilon,h)=|\varepsilon|^{s(2q)-2qs}w_{iq}((h/|\varepsilon|^{1/\varphi})^{2q}). \quad (14)$$

It can be shown in a very similar way that multifractal moments in the conducting phase obey the scaling form of

$$W_{cq}(\varepsilon,h)=\varepsilon^{t(2q)}w_{cq}((h/|\varepsilon|^{1/\varphi})^{2q}). \quad (15)$$

The only important difference in derivation of Eq. (15) is that we should start from expansion of $W_{cq}$ rather than $M_{cq}$ since the former for $h=0$ is defined both for $\varepsilon<0$ and $\varepsilon>0$; $W_{cq}(\varepsilon<0,0)=0$, $W_{cq}(\varepsilon>0,0)\sim\varepsilon^{t(2q)}$.

Eventually let us note that to include the dependence of $W_{iq}$ and $W_{cq}$ on $L$ in the thermodynamic limit the right-hand side of Eqs. (14) and (15) should be multiplied by the factor of $L^{d-2q}$.

## IV. VOLTAGE DISTRIBUTION IN THE TWO-COMPONENT RRN

In the previous section the new scaling functions of multifractal moments were derived. They enable us to write the multifractal moments as series expanded in the neighborhood of the point $h=0$ which is the well-studied case of RRSN for moments $W_{iq}$ or RRN for moments $W_{cq}$. Namely

$$W_{iq}(\varepsilon,h)\sim L^{d-2q}|\varepsilon|^{s(2q)-2qs}\left(1+\sum_{k=1}^{\infty}C_{kq}(h/|\varepsilon|^{1/\varphi})^{2qk}\right). \tag{16}$$

This expansion, which is valid for $L\to\infty$, affects the dependence of $W_{iq}$ on system size $L$ for $L<\xi$. The latter can be obtained by the usual finite-size scaling argument. Placing $|\varepsilon|=\xi^{-1/\nu}=L^{-1/\nu}$ in Eq. (16) and with the help of Eq. (10) we get

$$W_{iq}(L,h)\sim L^{\zeta(2q)}\left(1+\sum_{k=1}^{\infty}C_{kq}(hL^{1/(\nu\varphi)})^{2qk}\right). \tag{17}$$

The latter tells us that in the two-component RRN moments of voltage distribution in the insulating phase scale mostly like in the RRSN [see Eq. (8)]. The influence of the metallic component appears as the very small correction of order $(hL^{1/(\nu\varphi)})^{2q}$. In the following we will show that this small correction results from the distribution of voltage drops which is, however, very different from that of RRSN.

To proceed let us note that like in the case of RRN or RRSN the asymptotic form of the distribution $N_i(y)$ of the logarithm of voltage drops on insulating bonds, $y=-\ln(v^2)$, may be obtained via the inverse Laplace transform of moments $W_{iq}$ (Ref. 9),

$$N_i(y)=\mathscr{L}^{-1}[W_{iq}]=\mathscr{L}^{-1}[C_{0q}L^{\zeta(2q)}]+\sum_{k=1}^{\infty}\mathscr{L}^{-1}[C_{kq}h^{2qk}L^{\zeta(2q)+2qk/(\nu\varphi)}].$$

The first term in the sum above leads to the distribution $N_{\mathrm{RRSN}}(y)$ as it was shown for RRSN [see Eqs. (8) and (11)]. The inverse Laplace transforms of the next terms

$$\mathscr{L}^{-1}[C_{kq}h^{2qk}L^{\zeta(2q)+2qk/(\nu\varphi)}]=\frac{1}{2\pi j}\int_{-j\infty}^{+j\infty}dq\exp[\ln C_{kq}+2qk\ln(hL^{1/(\nu\varphi)})+\zeta(2q)\ln L+qy]\equiv N_{ik}(y), \tag{18}$$

where $j^2=-1$, can be calculated by the saddle-point approximation. If we assume that $C_{kq}$ depends weakly on $q$, the argument in the exponential is extremum for a value of $y$ such that

$$2k\ln(hL^{1/(\nu\varphi)})+\frac{\partial\zeta(2q)}{\partial q}\ln L+y=0,$$

or a value of $\alpha=y/\ln L$ such that

$$\alpha=-\frac{2k\ln(hL^{1/(\nu\varphi)})}{\ln L}-\frac{\partial\zeta(2q)}{\partial q}.$$

As $L$ increases the extremum value of the argument in the exponential approaches the form of the spectrum $\phi$ shifted by amount of $2k\ln(hL^{1/(\nu\varphi)})/\ln L$ on the $\alpha$ axis

$$\ln C_{kq}+\zeta(2q)\ln L-q\frac{\partial\zeta(2q)}{\partial q}\ln L\to\phi\left(\alpha+\frac{2k\ln(hL^{1/(\nu\varphi)})}{\ln L}\right)\ln L,\quad \text{for } 1\ll L<\xi.$$

Hence the distribution

$$N_{ik}(y)=a_kL^{\phi(\alpha+2k\ln(hL^{1/(\nu\varphi)})/\ln L)},$$

where $a_k=a_k(\alpha,\ln L)$ depends weakly on $\ln L$.[9] Eventually the asymptotic form of the distribution $N_i(y)$

$$N_i(y)=a_0L^{\phi(\alpha)}+a_1L^{\phi(\alpha+2\ln(hL^{1/(\nu\varphi)})/\ln L)}+a_2L^{\phi(\alpha+4\ln(hL^{1/(\nu\varphi)})/\ln L)}+\cdots. \tag{19}$$

As we have mentioned above, the distribution $N_i(y)$ is approached as $L$ increases but is still in the fractal region, i.e., $L<\xi$ ($\xi\sim h^{-\nu\varphi}$ in the two-component RRN). As we see the distribution $N_i(y)$ is composed of a number of subdistributions $N_{ik}(y)$ which are subsequently shifted by $2\ln(hL^{1/(\nu\varphi)})$ on the $y$ axis. Each of these subdistributions is governed by the spectrum $\phi$. In the following we will call the distributions $N_{ik}(y)$ the member distributions.

The distribution of voltage drops in the conducting phase can be obtained in a similar way. Note, however, that expansion of $W_{cq}(\varepsilon,h)$ about $h=0$ and for $\varepsilon>0$ is different from that for $\varepsilon<0$. This is because $W_{cq}(\varepsilon>0,0)\sim\varepsilon^{t(2q)}$ whereas $W_{cq}(\varepsilon<0,0)=0$. Thus the first term of the expansion, i.e., $W_{cq}(\varepsilon,0)$, appears or vanishes depending on the sign of $\varepsilon$. This of course has an effect in the finite-size behavior of $W_{cq}$ for $L<\xi$, i.e.,

$$W_{cq}(L,h)\sim L^{-p(2q)/\nu}\left(B_{0q}+\sum_{k=1}^{\infty}B_{kq}(hL^{1/(\nu\varphi)})^{2qk}\right), \tag{20}$$

where $B_{0q}$ appears or vanishes depending on whether the percolating cluster exists or not. The inverse Laplace trans-

form technique applied to moments $W_{cq}$ gives the distribution of the logarithm of voltage drops in the conducting phase

$$N_c(y)=\sum_{k=0}^{\infty} N_{ck}(y)=\sum_{k=0}^{\infty} b_k L^{f(\alpha+2k\ln(hL^{1/(\nu\varphi)})/\ln L)}, \quad (21)$$

where $b_k=b_k(\alpha,\ln L)$ depends weakly on $\ln L$ and $b_0=0$ if the percolation cluster does not exist. The form of Eq. (21) is approached for $L\gg 1$ but still $L<\xi$. Like in the insulating phase the distribution $N_c(y)$ is a sum of member distributions $N_{ck}(y)$ shifted subsequently by $2\ln(hL^{1/(\nu\varphi)})$ on the $y$ axis. However, unlike in the insulating phase, each member of the sum is governed by the multifractal spectrum $f(\alpha)$ obtained originally for RRN rather than by the spectrum $\phi(\alpha)$.

Having the distributions in both insulating and conducting components described we are able to write the distribution of the logarithm of voltage drops in the two-component RRN

$$N(y)=N_i(y)+N_c(y)=\sum_{k=0}^{\infty}[N_{ck}(y)+N_{ik}(y)]. \quad (22)$$

The distribution $N(y)$ has a ''multipeak'' structure in which the distributions $N_{\mathrm{RRN}}(y)$ and $N_{\mathrm{RRSN}}(y)$ obtained for RRN and RRSN are rescaled and repeated with a period $2\ln(hL^{1/(\nu\varphi)})$ on the $y$ axis.

In the next section an alternative derivation of $N(y)$ is supplied. While much simpler, it is based however on the hierarchical model of the two-component RRN and thus has less general meaning. In the section after the next, computer simulations performed on 3D TCRRN are presented in order to check the predictions of scaling analysis given above.

## V. HIERARCHICAL MODEL

Recently the very useful and powerful hierarchical model of the two-component percolating system has been proposed.[17,23] In the model conductance $G_c$ in Fig. 1 represents metallic (first) component whereas conductance $G_i$ represents the ''insulating'' (second) component. It is assumed

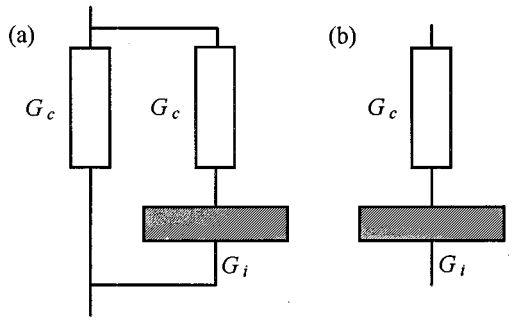


FIG. 1. Hierarchical model of the two-component random percolating system. Figures represent the first level of generation in case when (a) percolation cluster exists, (b) percolation cluster does not exist. In the next steps of generation conductance $G_c$ which is in series with $G_i$ is replaced by a branch as in Fig. 1(a).

that at the percolation threshold and for $L<\xi$, $G_c\sim g_c L^{-p(2)/\nu}$ and $G_i\sim g_i L^{\zeta(2)}$ as in Eqs. (3) and (8), respectively. The existence or not of the percolating cluster manifests itself only at the first level of iteration as it is shown in Fig. 1. In order to derive the voltage distribution let us assume that voltages appearing inside elements $G_c$ and $G_i$ obey the distributions $N_{\mathrm{RRN}}(y)$ and $N_{\mathrm{RRSN}}(y)$, respectively. If a constant voltage $V$ biases the structures in Fig. 1 the voltages appearing on elements $G_c$ are $V_{0c}=V$ and $V_{1c}\cong VG_i/G_c$ when a percolation cluster exists [Fig. 1(a)] or $V_{1c}\cong VG_i/G_c$ if it does not exist [Fig. 1(b)]. It is because in the $h\to 0$ limit we have $g_i\ll g_c$ and also $G_i\ll G_c$. Voltages on elements $G_i$ are $V_{0i}\cong V$ in either cases. In the second step of generation element $G_c$ which is in series with $G_i$ is replaced by the whole branch like those in Fig. 1(a). Consequently voltages that appear on new elements $G_c$ and $G_i$ are $V_{2c}\cong V_{1c}G_i/G_c$ and $V_{1i}\cong V_{1c}$. At the $k+1$ level of generation new voltages of $V_{(k+1)c}\cong V_{kc}G_i/G_c\cong V(G_i/G_c)^{k+1}$ and $V_{ki}\cong V_{kc}\cong V(G_i/G_c)^k$ appear on elements added in this level. In each of the elements voltages obey the distribution $N_{\mathrm{RRN}}(-\ln(V_b^2/V_{(k+1)c}^2))$ for elements $G_c$ or $N_{\mathrm{RRSN}}(-\ln(V_b^2/V_{ki}^2))$ for elements $G_i$. Thus the total distribution is the sum of all the contributions added during the generation

$$N(y)=\sum_{k=0}^{\infty} N_{\mathrm{RRN}}(-\ln(V_b^2/V_{kc}^2))+N_{\mathrm{RRSN}}(-\ln(V_b^2/V_{ki}^2))$$

$$=\sum_{k=0}^{\infty} N_{\mathrm{RRN}}(-\ln(V_b^2/V^2)+\ln(V_{kc}^2/V^2))+N_{\mathrm{RRSN}}(-\ln(V_b^2/V^2)+\ln(V_{ki}^2/V^2))$$

$$=\sum_{k=0}^{\infty} N_{\mathrm{RRN}}[y+2k\ln(G_i/G_c)]+N_{\mathrm{RRSN}}[y+2k\ln(G_i/G_c)]=\sum_{k=0}^{\infty} N_{\mathrm{RRN}}[y+2k\ln(hL^{1/(\nu\varphi)})]+N_{\mathrm{RRSN}}[y+2k\ln(hL^{1/(\nu\varphi)})]$$

$$=\sum_{k=0}^{\infty} b_0 L^{f(\alpha+2k\ln(hL^{1/(\nu\varphi)})/\ln L)}+a_0 L^{\phi(\alpha+2k\ln(hL^{1/(\nu\varphi)})/\ln L)},$$

where we have made use of relation $p(2)/\nu+\zeta(2)=(t+s)/\nu=1/(\nu\varphi)$ as given by Eqs. (4) and (10). Thus the periodic multipeak structure of voltage distribution is derived again. Note, however, that unlike the derivation based on the scaling assumption this derivation predicts constant amplitudes of subsequent member distributions which build up the total distribution. Let us also note that like the previous one, the present analysis predicts vanishing or not of the first term in the distribution $N_c$. This is obvious if we look at Fig. 1 where different first level generators are assumed depending on whether the percolating cluster exists or does not. Let us eventually note that more detailed treatment of the problem is possible if we use the new model of two-phase systems working inside the smearing region,[27] i.e., for $|\varepsilon|<h^{\varphi}$ instead of the model of Fig. 1.[28]

## VI. NUMERICAL SIMULATIONS

To test results obtained in the previous sections we have performed computer simulations of the 3D TCRRN. In each computational step a simple cubic lattice of linear size $L$, in which bonds were occupied randomly with probability $p$ by conductance $g_c=1$ was generated. The remaining bonds take value $g_i=h$. Once the lattice was generated, conductances of all the bonds were stored in a band matrix of network equations and unit dc external voltage $V=1$ was applied to the opposite sides of the lattice. Free boundary conditions were assumed in the remaining two directions. Next, voltages of all nodes in the lattice were computed by solving the matrix of network Kirchhoff's equations. To solve it, unlike in usual percolation problems, we have used a direct method of solving matrix linear equations. It is because we have found indirect methods not convergent in the case when conductances of the components that build the TCRRN differ by many orders of magnitude.

Indirect methods in each iteration improve voltages at every node of the lattice by a small amount which is calculated to balance the currents in every node. If the network contains conductances which differ by several orders of magnitude, e.g., it contains conductances of $1S$ and $1nS$ the balance is determined correctly provided all the voltages are determined very accurately (with $10^{-9}$ precision in our example). If they are not, *the error in current* which flows through the large conductance ($1S$) may exceed the current in the small one ($1nS$) and the node voltage is corrected in the wrong direction. The iteration procedure is not convergent. Thus we are forced to use a direct method. Since our matrix is positive and symmetrical (network matrix) we choose the Cholesky-Banachiewicz method.[29]

Once the matrix was solved and node voltages were determined, the voltages on all bonds in the lattices were calculated and their populations were gathered into bins separately for bonds $g_c$ and $g_i$. Three bins per voltage decade have been found sufficient enough to reveal the properties of voltage distribution. To make the data more visible we have used the distribution of energies dissipated in the network rather than the distribution of network voltages itself. It is because the distribution of network energies $P(-\ln e)=P_i(-\ln e)+P_c(-\ln e)=N_i(-\ln(e/h))+N_c(-\ln e)=N_i(-\ln e+\ln h)+N_c(-\ln e)$, takes a more familiar form in which the part $P_i$ of the distribution is shifted by $\ln h$ and thus does not overlap the $P_c$ part of the total distribution.

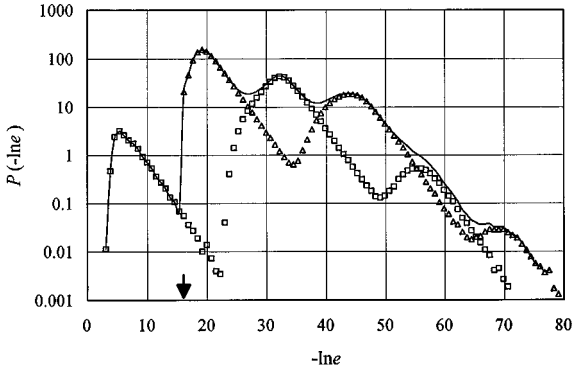


FIG. 2. The distribution $P(-\ln e)$ (solid line) of the logarithm of energy dissipated in the two-component RRN of size $L=8$, with $g_c=1$ and $g_i=h=10^{-7}$. Points refer to energies dissipated in metallic bonds (□) distribution $P_c$, and insulating bonds (△) distribution $P_i$. Solid line is the sum of the two. The arrow is placed at $-\ln e=-\ln h$.

We have performed simulations for various values of parameter $h=10^{-9}$, $10^{-7}$ and for various values of the lattice size $L=8,10,12,15$. For each pair of these parameters fixed, from several hundred for $L=15$ to several thousands for $L=8$ of network realizations were generated and distributions $P(-\ln e)$ were averaged. In Fig. 2 the distribution $P(-\ln e)$ versus $-\ln e$ for $h=10^{-7}$ and $L=8$ is shown. The multipeak structure of $P$, $P_i$, and $P_c$ is evident. The distributions are composed of several peaks shifted on the $-\ln e$ axis.

The first peak in $P$ or/and $P_c$ is related to the spectrum $f(\alpha)$. When rescaled, i.e., redrawn in coordinates $\ln P/\ln L=\ln P_c/\ln L$ versus $-\ln e/\ln L=-\ln(v^2)/\ln L$, as shown in Fig. 3, it asymptotically takes the shape of spectrum $f(\alpha)$ widely known in the percolation literature[3,7–14] (however mostly for $d=2$ dimensions). The collapse of the high-voltage part of the spectrum for different $L$ is easily seen. The calculated corresponding exponents $p(2q)/\nu$ for $q=0,1,2,3$ together with results from other simulations for comparison are summarized in Table I. For the low-voltage part (large $\alpha$) data do not collapse due to finite-size correction of order $1/\ln L$.[30] The slope of the low-energy part of the spectrum is approximately 0.3 for $L=15$ in quite good agreement with nearly the same value found by Duering and Bergman.[13]

The second peak in $P$ (or first in $P_i$) is related to spectrum $\phi(\alpha)$. This peak, however, is shifted on the $-\ln e$ axis by $-\ln h$ as is indicated by the arrow in Fig. 2. This is due to the quantity being used, i.e., $-\ln e$ instead of $-\ln(v^2)$ as we discussed above. The shape of the spectrum $\phi(\alpha)$ determined by rescaling data like those in Fig. 2 is shown in Fig. 4. We have not found any results with spectrum $\phi(\alpha)$ determined, to refer to for comparison. Only exponents for multifractal moments for $q=1$, 2, and 3 were calculated and thus can be compared with our results. This is done in Table II. As for the spectrum $f(\alpha)$, the collapse of the data as well as agreement of calculated exponents is really good, making our estimates quite reasonable.

All the following peaks in $P$ in Fig. 2 arise as a feature of

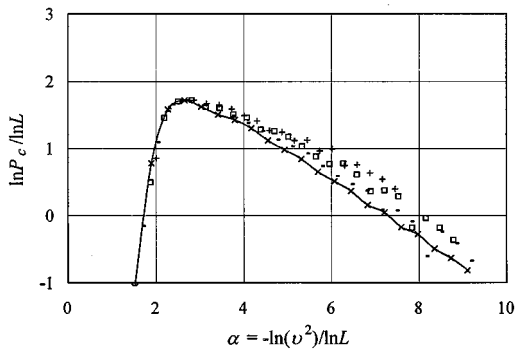


FIG. 3. Spectra $\ln P_c/\ln L$ of fractal dimensions describing the scaling of voltage distribution in RRN of size $L$. The spectra are obtained by the use of the data like those in Fig. 2 for various values of network size $L=8(\times)$, 10 $(-)$, 12 $(\square)$, 15 $(+)$. Only data which build up the first peak in $P$ (or/and $P_c$) in Fig. 2 were used. Data for different $L$ were adjusted to match $D_B=1.72$ in the apex. The value $\upsilon^2$ used on the horizontal axis is obtained as $\upsilon^2=e$. The collapse of data in high-voltage part (small $\alpha$) is excellent. For low-voltage part (large $\alpha$) data do not collapse due to finite-size correction of order $1/\ln L$. For $1\ll L<\xi$ the spectra reach the asymptotic form of $f(\alpha)$. The line for $L=8$ is drawn to guide the eye.

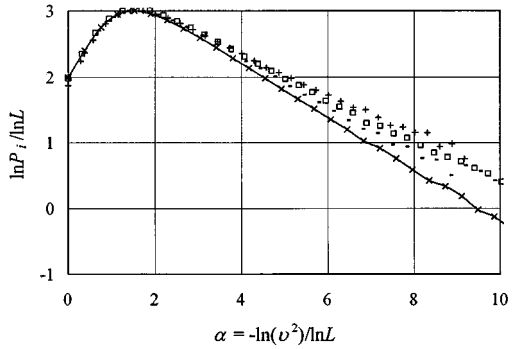


FIG. 4. Spectra $\ln P_i/\ln L$ of fractal dimensions describing the scaling of voltage distribution in RRSN of size $L$. The spectra are obtained by the use of the data like those in Fig. 2 for various values of network size $L=8(\times)$, 10 $(-)$, 12 $(\square)$, 15 $(+)$, and for $h=10^{-9}$. Only data which build up the second peak in $P$ (or first in $P_i$) were used. The values $\upsilon^2$ used on horizontal axis are obtained as $\upsilon^2=e/h$. For $1\ll L<\xi$ the spectra reach their asymptotic form of $\phi(\alpha)$. Spectra for different $L$ are shifted in vertical direction so that their maxima coincide with $\phi=d=3$. The line for $L=8$ is drawn to guide the eye.

the TCRRN. It is interesting that the contribution of the second peaks in both $P_i$ and $P_c$ is immense. The further peaks in $P_i$ and $P_c$ are merely visible and this means that magnitudes $a_k$ and $b_k$ in the expansions of Eqs. (19) and (21) are relatively small for $k\geqslant 2$. To measure the shift by which subsequent peaks in $P_i$ and $P_c$ are moved we rescaled data for various values of $h$ and $L$. In Fig. 5 results of simulations for constant $h=10^{-7}$ and two values $L=15$ and $L=8$ are shown. As expected the shifts of the second peaks in both $P_i$ and $P_c$ are different for different $L$. Note, however, that if Eqs. (19) and (21) hold, these (second) peaks should collapse if displayed in coordinates $\ln P_c/\ln L$ versus $(-\ln e+2\ln(hL^{1/(\nu\varphi)}))/\ln L$ for the distribution of energy dissipated in the metallic phase or in coordinates $\ln P_i/\ln L$ versus $(-\ln e+\ln h+2\ln(hL^{1/(\nu\varphi)}))/\ln L$ for the distribution of energy dissipated in the insulating phase. In Fig. 6 the test of data collapse is performed. In rescaling we have used recently estimated values of exponents $t/\nu=2.2$ (Ref. 33) and $s/\nu=0.85$ (Ref. 34), which give $1/(\nu\varphi)=3.05$ by the transfer-matrix technique. The agreement is excellent for the high-energy part of the distributions (small values of $-\ln e$), whereas much worse for small energies (large values of $-\ln e$). This slow convergence of the low-energy part of the spectrum will be discussed in the next section. The above rescaling tests only the $L$ dependence of the distributions. To test the $h$ dependence quite similar rescaling was performed. Data for constant $L=8$ and two various values of $h=10^{-9}$ and $h=10^{-7}$ as shown in Fig. 7, are rescaled also in Fig. 6. Here the data collapse is observed for the whole spectrum not only for the high-energy part of the distributions.

In Secs. IV and V it was concluded that distributions of voltage drops in the case when percolation cluster exists and when it does not exist differ merely in the existence or not of the first peak in $P_c$. The rest of these distributions should be the same. We test this numerically. Voltage distributions for percolating/nonpercolating samples were gathered sepa-

TABLE I. Exponents $-p(2q)/\nu$ for $q=0,1,2,3$ calculated by the use of the data which form the spectrum $f(\alpha)$ in Fig. 3, compared with results from other simulations. Exponents were calculated by power-law scaling of the multifractal moments $W_{cq}$ as a function of lattice size $L$.

| | Our result | Other sources |
|---|---|---|
| $-p(0)/\nu$ | 1.72 | 1.74 [a] |
| $-p(2)/\nu$ | −1.22 | −1.29, [b] −1.20, [c] −1.21, [d] −1.25, [f] −1.2 [g] |
| $-p(4)/\nu$ | −3.80 | −3.80, [b] −3.67, [c] −3.77, [d] −3.80, [e] −3.83 [f] |
| $-p(6)/\nu$ | −6.42 | −6.50, [b] −6.05, [c] −6.36 [f] |

[a]Reference 31.
[b]Reference 13.
[c]Reference 19 (deduced from exponents $x_q$).
[d]Reference 32.
[e]Reference 22.
[f]Reference 18 (deduced from exponents $x_q$).
[g]Reference 33.

TABLE II. Exponents $\zeta(2q)$ for $q=0,1,2,3$ calculated by the use of the data which form the spectrum $\phi(\alpha)$ in Fig. 4, compared with the results from other simulations. Exponents were calculated by finite-size scaling of the moments $W_{iq}(L,h)$.

| | Our result | Other sources |
|---|---|---|
| $\zeta(0)$ | 2.99 | |
| $\zeta(2)$ | 1.85 | 1.85, [a] 1.89, [c] 1.95 [d] |
| $\zeta(4)$ | 1.53 | 1.20, [b] 1.55, [c] 1.55 [d] |
| $\zeta(6)$ | 1.43 | 1.42, [c] 1.3 [d] |

[a]Reference 34.
[b]Reference 22.
[c]Reference 19 (our exponents $\zeta(2q)$ are exponents $-z_q$ of Ref. 19).
[d]Deduced from exponents $y_q$ of Ref. 18.

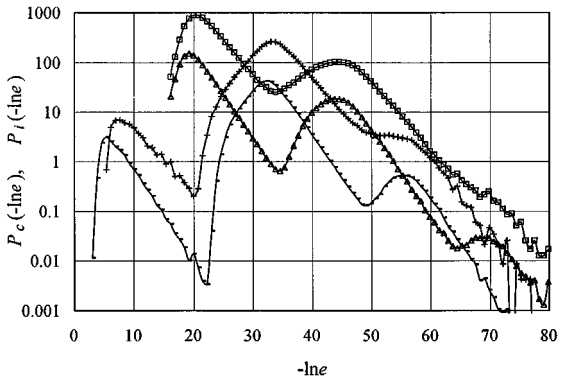


FIG. 5. Distributions $P_c$ and $P_i$ of the local power dissipated in metallic and insulating phases, respectively, for the TCRRN with $h=10^{-7}$ and various values of network size $L$. Data are for TCRRN of size $L=8$, (−) and (△), and for $L=15$, (+) and (□), respectively. Lines are drawn to guide the eye.

rately. They are shown in Fig. 8. Indeed the major difference between the distributions is the absence of the first (highly energetic) peak in $P_c$ when percolating cluster does not exist. Apart from this, data generally collapse especially for the high-energy parts of subsequent peaks. The differences that emerge in the low-energy parts of the peaks arise in our

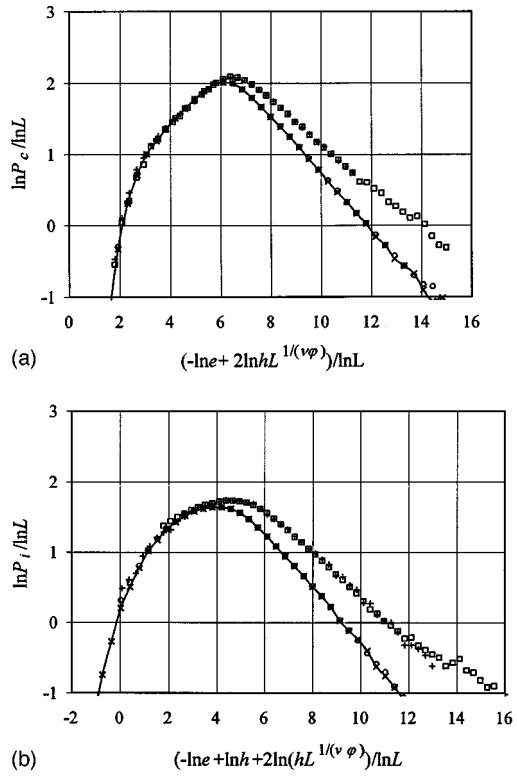


FIG. 6. Tests of collapsing of data from Figs. 5 and 7. Only data which build (a) the second peak in $P_c$, (b) the second peak in $P_i$, are used. Points refer to TCRRN with parameters $h=10^{-9}$, $L=15$ (□), $h=10^{-7}$, $L=15$ (+), $h=10^{-9}$, $L=8$ (×) and $h=10^{-7}$, $L=8$ (○). Lines for $L=8$ are drawn to guide the eye. Data for $L=8$ were shifted upward to match the high-energy part of the distributions for $L=15$. In rescaling the value of $1/(\varphi\nu)=(t+s)/\nu=3.05$ was used (see text).

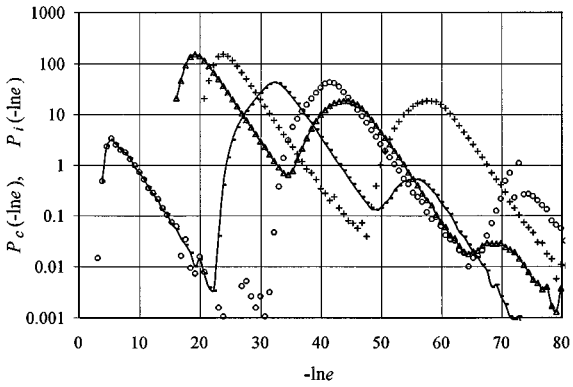


FIG. 7. Distributions $P_c$ and $P_i$ of the local power dissipated in metallic and insulating phases, respectively, for the TCRRN of size $L=8$. Data are for networks with $h=10^{-7}$, (−) and (△), and for $h=10^{-9}$, (○) and (+), respectively. Lines for $h=10^{-7}$ are drawn to guide the eye.

opinion for two reasons. The first one has the same origin that causes the rather poor collapse of the low-energy parts of all the spectra, and will be discussed in the next section. The second one may arise from different populations of percolating/nonpercolating samples (we observe approximately 2/3 of nonpercolating samples in the whole population) which make the statistical fluctuations in the distributions different.

## VII. DISCUSSION AND SUMMARY

The distribution of voltage drops in the two-component RRN has a multipeak structure. It is built up from subsequent member distributions shifted on the voltage axis. This was predicted theoretically by scaling analysis and analysis of the hierarchical model of the two-component random system. Numerical simulations performed on 3D TCRRN confirm this prediction. The collapsing of data is very good but only

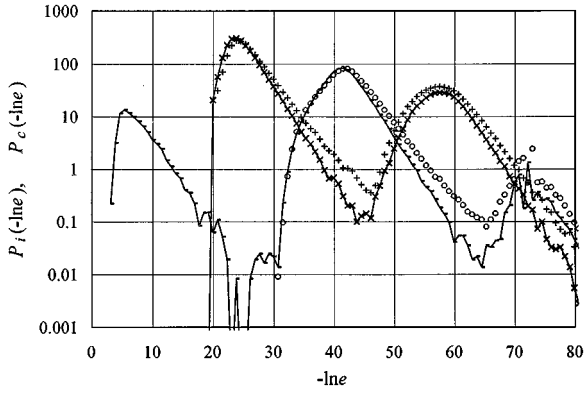


FIG. 8. Distributions $P_c$ and $P_i$ of the local power dissipated in metallic and insulating phases, respectively, for the two-component RRN of size $L=10$ and with $h=10^{-9}$. Points refer to percolating samples, (−) and (×), and to nonpercolating samples, (○) and (+), respectively. Lines for percolating samples are drawn to guide the eye. The populations of percolating/nonpercolating samples used in calculations are 481 and 1029, respectively.

for high-energy parts of subsequent members of the distribution. Collapsing is much worse for the low-energy parts of these members. A similar effect was observed in classical multifractal analysis in RRN. It was caused by the breakdown of power-law scaling for negative multifractal moments; for $q<0$ moments $W_q$ do not scale in the power-law manner of Eqs. (3) and (8). Instead exponential decay of the smallest current in the network was observed. This results in the scaling form of $M_q \sim \exp[(-\beta+q\chi)L^{\rho}]$ for $q<0$.[8,35,36] The influence of this effect on the shape of multifractal spectrum $f(\alpha)$ is still the subject of controversy and different scenarios for the behavior of $f(\alpha)$ for large $\alpha$ have been recently proposed.[10,11,30]

Theoretical analyses performed in Secs. III, IV, and V predict a semiperiodic structure of voltage distribution in which multifractal spectra $f(\alpha)$ and $\phi(\alpha)$ are repeated with the period of $2\ln(hL^{1/(\nu\varphi)})/\ln L$. However, numerical simulations show the subsequent peaks are not only shifted on the $y$ axis but also have different shapes, especially near their maxima. This is a new effect which may suggest that new sets of independent exponents appear in our system. Below we discuss this problem in a more detailed way.

First let us note that the above effects can be explained and understood better in terms of qualitative analysis of transport processes which take place in the TCRRN. The first peak in the distribution $N_c$ is related to currents flowing in the backbone of the percolating cluster. If $g_i>0$ currents start flowing in the insulating phase. The first peak in $N_i$ describes their distribution. This is, however, not the only effect. The other is that dangling ends and isolated metallic clusters, which in ideal ($g_i=0$) RRN carry no currents, now carry currents that flow through the insulating phase. Thus they are of order $h$. This is the origin of the second peak in $N_c, N_{c1}$. Thus it turns out that $N_{c1}$ describes also the distribution of voltage drops in dangling ends, isolated clusters and all other metallic bonds which are ''wetted'' by currents when insulating phase takes finite value, $g_i>0$. It is obvious that they form a percolation object different from percolating cluster. Thus it is not surprising that $N_{c0}$ and $N_{c1}$ have different shapes especially near the apex where the influence of the geometry of the percolation object is the most significant. Similarly $N_{i1}$ is the distribution of voltage drops on bonds which form the perimeter of metallic clusters, i.e., bonds which in RRSN never carry currents since they lie on surface of superconducting medium and thus are biased by zero voltage. In case of two-component RRN they start carrying currents due to nonzero voltages on non-ideal-superconducting bonds. Similar qualitative explanation of further peaks in $N_i$ and $N_c$ is also possible.

Were thus the analyses given in Secs. III, IV, and V wrong? To answer let us recall that multifractal moments $M_q$ and $W_q$ introduced in Sec. II are defined *only for current carrying bonds*. This fact is obvious if we realize that, for example, the scaling of zero-order moment $M_0$ is described by fractal dimension of the percolating backbone, $D_B$. Since multifractal moments, $M_{cq}$ and $W_{iq}$ introduced in the beginning of Sec. III are matched to moments $M_q$ and $W_q$ in the limit $h\to 0$, this means that $M_{cq}$ and $W_{iq}$ are defined for the same set of bonds for which moments $M_q$ and $W_q$ are defined. Now it is clear that our equation (21) describes, in fact, distribution of voltages only on metallic bonds belonging to the percolating backbone. Similarly Eq. (19) describes the distribution of voltages only on insulating bonds which do not lie on the surface of metallic clusters. The distribution of Eq. (22) would have been thus observed in our simulations of real TCRRN if we had used an algorithm which had counted only bonds belonging to the subsets of bonds described above. Our algorithm counts, however, all the bonds in the lattice. This is the reason why the shapes of subsequent member distributions obtained from the simulations are not similar to $f(\alpha)$ or $\phi(\alpha)$. The distribution $N_{c1}$ obtained in the simulations apart from the contribution, $N_{c1}^{\mathrm{BB}}$, coming from backbone bonds, i.e., $N_{c1}^{\mathrm{BB}} = b_1 L^{f(\alpha+2\ \ln(hL^{1/(\nu\varphi)}))}$, contains also the contribution, $N_{c1}^{\overline{\mathrm{BB}}}$, which comes from dangling ends and separate clusters. Similarly distribution $N_{i1}$ apart from the contribution, $N_{i1}^{\mathrm{BB}}$, coming from bonds which do not lie on the surface of metallic clusters, i.e., $N_{i1}^{\mathrm{BB}} = a_1 L^{\phi(\alpha+2\ \ln(hL^{1/(\nu\varphi)}))}$, contains also the contribution, $N_{i1}^{\overline{\mathrm{BB}}}$, which comes from bonds lying on the surface of metallic clusters. The distributions $N_{c1}^{\overline{\mathrm{BB}}}$ and $N_{i1}^{\overline{\mathrm{BB}}}$ appear on the $y$ axis in places where the distributions $N_{c1}^{\mathrm{BB}}$ and $N_{i1}^{\mathrm{BB}}$ are located, i.e., they are shifted towards low energies by $2\ln(hL^{1/(\nu\varphi)})$. These shifts are well understood as we have discussed above (see also the analysis in Sec. V).

Now the question arises, whether these new distributions, both $N_{c1}$, $N_{i1}$, and $N_{c1}^{\overline{\mathrm{BB}}}$ and $N_{i1}^{\overline{\mathrm{BB}}}$, scale or not, i.e., whether the multifractal formalism could be applied to describe their properties. The answer is not easy. On one hand, these distributions appear in the low-energy part on the $y$ axis where there is no scaling as we have mentioned in the beginning of this section. It is obvious that distributions $N_{i1}$ and $N_{c1}$ depend not only on the geometry of appropriate percolation object. For example the distribution of voltage drops in dangling ends depends not only on their geometry but also on the distribution of voltage drops in the percolating cluster as well as inside the insulating phase. Thus the distributions $N_{i0}$ and $N_{c0}$ are both involved in building $N_{i1}$ and $N_{c1}$. Now if we note that there is no scaling in the low-energy parts of $N_{i0}$ and $N_{c0}$ it may occur that there is no scaling not only in the low-energy parts of $N_{i1}$ or $N_{c1}$.

On the other hand, let us note that multifractal moments $M_{cq}$ for nonpercolating samples are determined mainly by the distribution $N_{c1}$ which in this case appears as the first peak in $N_c$ (see Fig. 8). The test of scaling of moments $M_{cq}$ for $q=1,2,3$ in this case has been already performed.[19] Now if we look at Fig. 8 where the shapes of the $N_{c1}$'s in percolating/nonpercolating samples are nearly the same, we may expect that in general positive moments calculated for the distribution $N_{c1}$ do scale. This means that multifractal formalism could be used to describe the high-energy part of $N_{c1}$. This is confirmed in view of our Figs. 6(a) and 6(b). Moreover exponents found in the test mentioned above[19] are $[-p(2q)+2q/\varphi]/\nu$ in agreement with our scaling analysis of Sec. IV. This means that the regions of $N_{c1}$ responsible for positive moments, has the same shape as the spectrum $f(\alpha)$. This may further mean that $N_{c1}$ has a structure in which either $N_{c1}^{\mathrm{BB}}$ is followed by $N_{c1}^{\overline{\mathrm{BB}}}$ or both $N_{c1}^{\mathrm{BB}}$ and $N_{c1}^{\overline{\mathrm{BB}}}$ have the fronts (high-energy parts) which scale like $L^{f(\alpha+2\ \ln(hL^{1/(\nu\varphi)})/\ln L)}$. Numerical simulations would certainly give some new arguments here.

Another question is, whether it is possible to solve the problem by redefinition of multifractal moments so that summation in the definitions in the beginning of Sec. III is extended from backbone bonds only over all current carrying bonds. This would lead directly to calculation of voltage distribution in TCRRN. Such a redefinition makes the range of $\alpha$ in which the distribution can be reconstructed limited. Note that in this case $q=0$ moments cannot be written in the form of Eqs. (14) or (15) and consequently expanded in a form of Eq. (17). Indeed, for example for $h=0$ we have $M_{c0}\sim L^{D_B}$ whereas for any $h>0$ in the limit $q\to 0$ we have $M_{c0+}\sim L^{d}$. If we, however assume that for $q\geqslant 1$ redefined multifractal moments do scale like those in Sec. III, the inverse Laplace transform is well defined only if the saddle point is located at $q$'s greater than 1, i.e., for values of $q$ for which

$$0<-\frac{\partial\zeta}{\partial q}<-\left.\frac{\partial\zeta}{\partial q}\right|_{q=1}\equiv\zeta_R'$$

or for a values of $\alpha$ for which

$$\frac{2k\ln(hL^{1/(\nu\varphi)})}{\ln L}<\alpha<\frac{2k\ln(hL^{1/(\nu\varphi)})}{\ln L}+\zeta_R'.$$

The latter describes intervals of $\alpha$ in which the high-energy parts of subsequent $N_{ck}$'s are located. This is consistent with our earlier remarks.

Finally let us refer to the results of other authors. Voltage distribution in TCRRN was calculated by Monte Carlo simulations of 2D square lattice in Ref. 16. Simulations were performed for the values of $h=0.001$ and $L=100$. In 2D we have $\varphi\nu\cong 0.5$[1] and $\xi\cong h^{-\nu\varphi}\cong 32<L=100$ and this means that voltage distribution in homogeneous rather than in fractal region was calculated. In the homogeneous region the distribution is quite different; i.e., it is a $\delta$ function peaked at a value of voltage equal to $L^{d-1}$. Thus for the values of $h$ and $L$ used in the simulations a multipeak structure of the distribution (which is valid in fractal region) starts changing toward a single $\delta$ function as was discussed in Ref. 37. The authors displayed voltage distribution directly, i.e., versus $\ln\upsilon$ on the horizontal axis, so that overlapping of $N_c$ and $N_i$ takes place. Nevertheless it is possible to distinguish between fronts of $N_c$ and $N_i$ in the histograms. One cannot find further peaks in $N_{\mathrm{TCRRN}}$, due to collapsing of all the peaks in the homogeneous region.

Very recently Monte Carlo simulations of current distribution in 2D TCRRN has also been performed.[24] The authors have obtained a fine two-peak structure (in case of current distribution overlapping does not occur). In this case simulations were performed for $h=0.0001$ and $L=60$, i.e., in the fractal region since $\xi\cong 100>L=60$. In spite of this the shift by which $N_{c1}$ is expected to be moved on $\ln i$ axis is only of 1.02 which means that in fact $N_{c0}$ and $N_{c1}$ (and $N_{c2}$ which is shifted by 2.04) do overlap each other and form one common peak. The same is for $N_{i0}$ and $N_{i1}$ and $N_{i2}$ and thus only two peaks in the whole distribution are observed. The authors have also fitted the small current part of the calculated distribution by Gaussian. Good agreement was found. They were prompted to make this approximation by their earlier derivation of current distribution in a hierarchical diamond lattice which consisted of two types of conductance. In this case they have found such an approximation reasonable, despite that several peaks in the distribution calculated for $h=10^{-6}$ and $L=2^8$ are also visible. The authors, however, clearly stated that one should take the analogy between real TCRRN and hierarchical diamond lattice with caution. In view of our present results this remark is essential. We do not think that distribution of currents flowing in real TCRRN could be Gaussian.

In summary the distribution of voltage drops in the two-component RRN has been described. It is composed of several peaks, the member distributions, shifted subsequently on $-\ln(\upsilon^2)$ axis by amount of $2\ln(hL^{1/(\nu\varphi)})$. Member distributions describe voltage drops in either the metallic phase—members $N_{ck}$, or in the insulating phase—members $N_{ik}$. The zero-order member of the $N_{ck}$ family is governed by the multifractal spectrum $f(\alpha)$ found originally for RRN. The zero-order member of the $N_{ik}$ family is governed the multifractal spectrum $\phi(\alpha)$ found originally for RRSN. The next members are built from two components. The first one is the scaled repetition of $N_{c0}$ for the $N_{ck}$ family or $N_{i0}$ for the $N_{ik}$ family. The other one is the distribution of voltage drops in such percolation objects like dangling ends, isolated clusters for the $N_{ck}$ family or clusters perimeter for the $N_{ik}$ family.

## ACKNOWLEDGMENTS

The author would like to thank P. Januszewski for the critical reading of the manuscript. The useful discussions with A. Kusy, A. A. Snarskii, P. Pusz, and W. Pusz are also gratefully acknowledged.

[1] D. Stauffer, *Introduction to Percolation Theory* (Taylor & Francis, London, 1985).
[2] L. de Arcangelis, S. Redner, and A. Coniglio, Phys. Rev. B **31**, 4725 (1985).
[3] L. de Arcangelis, S. Redner, and A. Coniglio, Phys. Rev. B **34**, 4656 (1985).
[4] R. Rammal, C. Tannous, P. Breton, and A.-M. S. Tremblay, Phys. Rev. Lett. **54**, 1718 (1985); R. Rammal, C. Tannous, and A.-M. S. Tremblay, Phys. Rev. A **31**, 2662 (1985).
[5] A. Coniglio, Phys. Rev. Lett. **46**, 250 (1981).
[6] B. Fourcade, P. Breton, and A.-M. S. Tremblay, Phys. Rev. B **36**, 8925 (1987).
[7] L. de Arcangelis, S. Redner, and A. Coniglio, Phys. Rev. B **36**, 5631 (1987).
[8] R. Blumenfeld, Y. Meir, A. Aharony, and A. B. Harris, Phys. Rev. B **35**, 3534 (1987).
[9] B. Fourcade and A.-M. S. Tremblay, Phys. Rev. B **36**, 2352 (1987).
[10] G. G. Batrouni, A. Hansen, and M. Nelkin, J. Phys. (Paris) **48**, 771 (1987); G. G. Batrouni, A. Hansen, and S. Roux, Phys. Rev. A **38**, 3820 (1988).
[11] B. Kahng, Phys. Rev. Lett. **64**, 914 (1990); A. Hansen, E. Hinrichsen, and S. Roux, Phys. Rev. Lett. **67**, 279 (1991); B. Kahng, *ibid.* **67**, 280 (1991).

[12] E. Duering, R. Blumenfeld, D. J. Bergman, A. Aharony, and M. Murat, J. Stat. Phys. **67**, 113 (1992).
[13] E. Duering and D. J. Bergman, J. Stat. Phys. **60**, 363 (1990).
[14] J. P. Straley, Phys. Rev. Lett. **39**, 4531 (1989).
[15] A. L. Efros and B. Shklovskii, Phys. Status Solidi B **76**, 475 (1976); J. P. Straley, J. Phys. C **9**, 783 (1976).
[16] L. de Arcangelis and A. Coniglio, J. Stat. Phys. **48**, 935 (1987).
[17] A. E. Morozovsky and A. A. Snarskii, Zh. Eksp. Teor. Fiz. Lett. **15**, 51 (1989); Zh. Eksp. Teor. Fiz. **95**, 1844 (1989).
[18] R. R. Tremblay, G. Albinet, and A.-M. S. Tremblay, Phys. Rev. B **43**, 11 546 (1991).
[19] R. R. Tremblay, G. Albinet, and A.-M. S. Tremblay, Phys. Rev. B **45**, 755 (1992).
[20] A.-M. S. Tremblay, R. R. Tremblay, G. Albinet, and B. Fourcade, Physica A **183**, 398 (1992).
[21] A. Kolek, Phys. Rev. B **45**, 205 (1992).
[22] A. Kolek, Int. J. Electron. **73**, 1095 (1992).
[23] A. E. Morozovsky and A. A. Snarskii, Zh. Eksp. Teor. Fiz. Lett. **18**, 74 (1992); Zh. Eksp. Teor. Fiz. **102**, 683 (1992).
[24] K. W. Yu and P. Y. Tong, Phys. Rev. B **46**, 12 137 (1992); **46**, 11 487 (1992); J. Phys. A **26**, L119 (1993); **26**, 4223 (1993).
[25] D. C. Wright, D. J. Bergman, and Y. Kantor, Phys. Rev. B **33**, 396 (1986).
[26] J. P. Straley, J. Phys. C **12**, 3711 (1979).
[27] A. A. Snarskii and A. E. Morozovsky, Int. J. Electron. **78**, 135 (1995).
[28] A. A. Snarskii (private communication).
[29] A. Björck and G. Dahlquist, *Numerical Methods* (Prentice-Hall, Englewood Cliffs, NJ, 1974).
[30] A. Aharony, R. Blumenfeld, and A. B. Harris, Phys. Rev. B **47**, 5756 (1993).
[31] H. J. Herrmann and H. E. Stanley, Phys. Rev. Lett. **53**, 1121 (1984).
[32] A. Kolek and A. Kusy, J. Phys. C **21**, L573 (1988).
[33] B. Derrida, D. Stauffer, H. J. Herrmann, and J. Vannimenus, J. Phys. (Paris) Lett. **44**, L701 (1983).
[34] H. J. Herrmann, B. Derrida, and J. Vannimenus, Phys. Rev. B **30**, 4080 (1984).
[35] In fact moments $M_q$ scale no longer as power laws for $q<q_c\leqslant 0$. Different threshold values of $q_c$ have been proposed. See also Refs. 30 and 10–14.
[36] A. Aharony, R. Blumenfeld, P. Breton, B. Fourcade, A. B. Harris, Y. Meir, and A.-M. S. Tremblay, Phys. Rev. B **40**, 7318 (1989).
[37] S. Roux and A. Hansen, Europhys. Lett. **8**, 729 (1989).